High-energy, near- and mid-IR picosecond pulses generated by a fiber-MOPA-pumped optical parametric generator and amplifier

Lin Xu,* Ho-Yin Chan, Shaif-ul Alam, David J. Richardson and David P. Shepherd

Optoelectronics Research Centre, University of Southampton, Southampton, SO17 1BJ, UK
**l.xu@soton.ac.uk*

Abstract: We report a high-energy picosecond optical parametric generator/amplifier (OPG/A) based on a MgO:PPLN crystal pumped by a fiber master-oscillator-power-amplifier (MOPA) employing direct amplification. An OPG tuning range of 1450-3615 nm is demonstrated with pulse energies as high as 2.6 μJ (signal) and 1.2 μJ (idler). When seeded with a ~100 MHz linewidth diode laser, damage-limited pulse energies of 3.1 μJ (signal) and 1.3 μJ (idler) have been achieved and the signal pulse time-bandwidth product is improved to ~2 times transform-limited. When seeded with a 0.3 nm-bandwidth filtered amplified spontaneous emission source, crystal damage is avoided and maximum pulse energies of 3.8 μJ (signal) and 1.7 μJ (idler) are obtained at an overall conversion efficiency of 45%.

OCIS codes: (190.4970) Parametric oscillators and amplifiers; (190.4400) Nonlinear optics, materials.

References and links

1. S. Woutersen, U. Emmerichs, and H. J. Bakker, "Femtosecond mid-IR pump-probe spectroscopy of liquid water: evidence for a two-component structure," Science **278**, 658-660 (1997).
2. M. R. Papantonakis, and R. F. Haglund Jr, "Picosecond pulsed laser deposition at high vibrational excitation density: the case of poly(tetrafluoroethylene)," Appl. Phys. A **79**, 1687-1694 (2004).
3. H. Linnenbank, and S. Linden, "High repetition rate femtosecond double pass optical parametric generator with more than 2 W tunable output in the NIR," Opt. Express **22**, 18072-18077 (2014).
4. F. Seifert, V. Petrov, and F. Noack, "Sub-100-fs optical parametric generator pumped by a high-repetition-rate Ti:sapphire regenerative amplifier system," Opt. Lett. **19**, 837-839 (1994).
5. J. Krauth, A. Steinmann, R. Hegenbarth, M. Conforti, and H. Giessen, "Broadly tunable femtosecond near- and mid-IR source by direct pumping of an OPA with a 41.7 MHz Yb:KGW oscillator," Opt. Express **21**, 11516-11522 (2013).
6. V. Z. Kolev, M. W. Duering, B. Luther-Davies, and A. V. Rode, "Compact high-power optical source for resonant infrared pulsed laser ablation and deposition of polymer materials," Opt. Express **14**, 12302-12309 (2006).
7. D. D. McAlevy Bubb, and R. F. Haglund, "Resonant infrared pulsed laser ablation and deposition of thin polymer films," in *Pulsed Laser Deposition of Thin Films*, R. Eason, ed. (John Wiley & Sons, Inc., 2006).
8. R. Piccoli, F. Pirzio, A. Agnesi, V. Badikov, D. Badikov, G. Marchev, V. Panyutin, and V. Petrov, "Narrow bandwidth, picosecond, 1064 nm pumped optical parametric generator for the mid-IR based on $HgGa_2S_4$," Opt. Lett. **39**, 4895-4898 (2014).
9. S. C. Kumar, M. Jelínek, M. Baudisch, K. T. Zawilski, P. G. Schunemann, V. Kubecek, J. Biegert, and M. Ebrahim-Zadeh, "Tunable, high-energy, mid-infrared, picosecond optical parametric generator based on $CdSiP_2$," Opt. Express **20**, 15703-15709 (2012).
10. G. Marchev, F. Pirzio, R. Piccoli, A. Agnesi, G. Reali, P. G. Schunemann, K. T. Zawilski, A. Tyazhev, and V. Petrov, "Narrow-bandwidth, ~100 ps seeded optical parametric generation in $CdSiP_2$ pumped by Raman-shifted pulses at 1198 nm," Opt. Lett. **38**, 3344-3346 (2013).
11. T. V. Andersen, O. Schmidt, C. Bruchmann, J. Limpert, C. Aguergaray, E. Cormier, and A. Tünnermann, "High repetition rate tunable femtosecond pulses and broadband amplification from fiber laser pumped parametric amplifier," Opt. Express **14**, 4765-4773 (2006).
12. F. Kienle, P. Siong Teh, S.-U. Alam, C. B. E. Gawith, D. C. Hanna, D. J. Richardson, and D. P. Shepherd, "Compact, high-pulse-energy, picosecond optical parametric oscillator," Opt. Lett. **35**, 3580-3582 (2010).
13. H. Y. Chan, S. U. Alam, L. Xu, J. Bateman, D. J. Richardson, and D. P. Shepherd, "Compact, high-pulse-energy, high-power, picosecond master oscillator power amplifier," Opt. Express **22**, 21938-21943 (2014).
14. O. Gayer, Z. Sacks, E. Galun, and A. Arie, "Temperature and wavelength dependent refractive index equations for MgO-doped congruent and stoichiometric $LiNbO_3$," Appl. Phys. B **91**, 343-348 (2008).
15. A. V. Okishev, and J. D. Zuegel, "Intracavity-pumped Raman laser action in a mid IR, continuous-wave (cw) MgO:PPLN optical parametric oscillator," Opt. Express **14**, 12169-12173 (2006).
16. T. Traub, F. Ruebel, and J. A. L'huillier, "Efficient injection-seeded kHz picosecond LBO optical parametric generator," Appl. Phys. B **102**, 25-29 (2011).
17. J. Prawiharjo, H. S. S. Hung, D. C. Hanna, and D. P. Shepherd, "Theoretical and numerical investigations of parametric transfer via difference-frequency generation for indirect mid-infrared pulse shaping," J. Opt. Soc. Am. B **24**, 895-905 (2007).
18. Y. Furukawa, K. Kitamura, A. Alexandrovski, R. K. Route, M. M. Fejer, and G. Foulon, "Green-induced infrared absorption in MgO doped $LiNbO_3$," Appl. Phys. Lett. **78**, 1970-1972 (2001).
19. B. Bourliaguet, V. Couderc, A. Barthélémy, G. W. Ross, P. G. R. Smith, D. C. Hanna, and C. De Angelis, "Observation of quadratic spatial solitons in periodically poled lithium niobate," Opt. Lett. **24**, 1410-1412 (1999).
20. P. Di Trapani, A. Bramati, S. Minardi, W. Chinaglia, C. Conti, S. Trillo, J. Kilius, and G. Valiulis, "Focusing versus defocusing nonlinearities due to parametric wave mixing," Phy. Rev. Lettt. **87**, 183902 (2001).

1. Introduction

Tunable sources of short laser pulses in the mid-IR are useful for a number of spectroscopic and materials processing applications due to the presence of characteristic vibrational absorptions of organic materials in this spectral region [1,2]. Optical parametric processes offer an effective route to frequency down-conversion of readily available near-IR sources to longer mid-IR wavelengths. In particular, optical parametric generators (OPGs) are attractive, due to their simple single-pass nature, allowing compact devices that are less costly and less sensitive to external perturbations in comparison to the synchronously-pumped cavities of short-pulse optical parametric oscillators (OPOs). However, as a result of the single-pass interaction, OPGs require high-intensity pump sources to achieve a high parametric gain. Typically, this has been achieved using solid-state near-IR pump lasers based on gain media such as Ti:sapphire or Yb-doped tungstates [3-5]. Additionally, in order to reach the μJ-level mid-IR pulse energies that are interesting for organic materials processing techniques such as resonant infrared pulsed laser deposition (RIR-PLD) [6,7], systems are normally operated at Hz to kHz repetition rates [8-10].

Advances in fiber laser technology have greatly extended the range of achievable output powers and energies from such devices, raising them to levels suitable for pumping parametric devices. As an example, an optical parametric amplifier (OPA) pumped by a fiber chirped-pulse amplification source has generated femtosecond pulses with energies as high as 1.2 μJ in the near-IR [11]. Using a 7.19 MHz, Yb-fiber MOPA system, employing similar direct amplification to the system described here, but with a more complex OPO configuration, pulse energies as high as 0.49 μJ at 1.5 μm and 0.19 μJ at 3.6 μm have been demonstrated with ~100 ps pulses [12].

Here we describe a compact, stable, OPG pumped by a nearly all-fiber MOPA system operating at 1035 nm, with 150 ps duration pulses at 1 MHz repetition rate and employing simple direct amplification. By injection-seeding with a narrow (~100MHz) linewidth continuous-wave (CW) laser for OPA operation, the pump threshold and output linewidth were significantly decreased and pulse energies as high as 3.1 μJ were obtained before damage was observed in the MgO:PPLN crystal. Using a broader 0.3 nm-bandwidth seed, maximum energies of 3.8 μJ signal (1541 nm) and 1.7 μJ idler (3150 nm) were obtained without crystal damage, limited only by the pump energy and at an overall power conversion efficiency of 45%.

2. Experimental setup

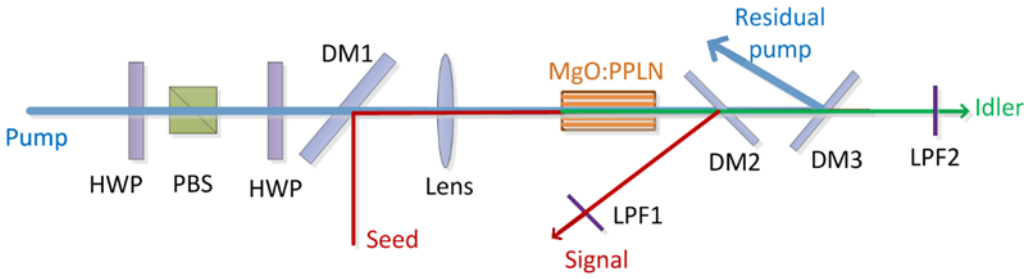

Fig. 1. Experimental setup of the OPG (unseeded) and OPA (seeded). HWP, half-wave plate; PBS, polarizing beam splitter; DM, dichroic mirror; LPF, long-pass filter.

The experimental setup is shown in Fig. 1. The MOPA pump source, which is described in detail in [13], consisted of a PM-fiber-pigtailed gain-switched laser-diode seed laser, self-seeded by feedback from a uniform-pitch fiber Bragg grating, operating at a central wavelength of 1035 nm and a repetition rate of 87.5 MHz, followed by two Yb-fiber preamplifier stages. A fiber pigtailed electro-optic modulator (EOM) was then used as a pulse-picker to reduce the repetition frequency to 1 MHz. A third 10-μm-core Yb-fiber preamplifier and a 25-μm-core Yb-fiber power booster were employed to increase the output power. The power input to the OPG/OPA was varied using a half-wave plate before a polarizing beam splitter, as shown in Fig. 1. Another half-wave plate was used to rotate the beam polarization orientation to realize quasi-phase matching in a MgO-doped periodically poled lithium niobate (PPLN) crystal. The beam after the dichroic mirror (DM1, Fig. 1) was focused into the PPLN with a beam waist of 80 μm in order to ensure that the peak intensity (<1GW/cm^2) was below the crystal damage threshold. The 40-mm-long PPLN crystal (MOPO1-1.0-40, Covesion) had five gratings with periods ranging from 29.5 to 31.5 μm in steps of 0.5 μm and was mounted inside an oven to allow temperature tuning in the range from 20 to 200 °C with a precision of 0.1 °C. The signal output was extracted using a dichroic mirror (DM2, Fig. 1), with high transmission at the pump and idler wavelengths and high reflection at the signal wavelength. The signal power was measured after a long-pass filter (LPF1, Fig. 1), which had a low-wavelength cut-off at 1250 nm (FEL1250, Thorlabs). After the unconverted pump was filtered by a dichroic mirror (DM3, Fig. 1), the idler beam then passed through a long-pass filter (LPF2, Fig. 1) with a low-wavelength cut-off of 1.9 μm (LWP-4047-1-1-09, Northumbria Optical Coatings) before the idler power was measured. The signal and idler output powers discussed in the following text correspond to that immediately after the PPLN crystal, taking into account the losses of the DMs and LPFs.

3. Results and discussion

The available average pump power from the MOPA system, after passing through the various optical elements before the PPLN crystal was 12 W. The pump pulses had a duration of 150 ps and a bandwidth of 0.5 nm, corresponding to a time-bandwidth product (TBP) of 20. Without seed laser injection, the generation of signal and idler pulses was observed at a pump threshold of around 5 W in the single-pass OPG process. By using different PPLN grating periods and oven temperatures, the signal (idler) wavelength could be tuned from 1450 nm to 1800 nm (2435 nm to 3615 nm), as shown in Fig. 2. The measured wavelengths are in accordance with the theoretically predicted curve based on the published Sellmeier data [14]. Figure 2 also describes the output power as a function of pump power. The signal and idler output powers increased linearly with slope efficiencies of 38% and 17.5%, resulting in maximum powers of 2.67 W and 1.24 W. Therefore, considering the total output power, the overall power conversion efficiency of the OPG was 32% at full power. For a grating with a period of 29.5 µm and a temperature of 150 °C, the measured signal and idler spectra had central wavelengths of 1504 nm and 3325 nm, respectively. The full-width at half-maximum (FWHM) spectral bandwidths of the signal and idler were 5.6 nm and 40 nm, respectively, as given in Fig. 3(a). The second peak located at 1510 nm in the signal spectrum under high-power OPG operation shown in Fig. 3(a), is attributed to a 1st stokes Raman frequency shift. The frequency shift of 46 cm^{-1} from 1500 nm is consistent with the published value for MgO:PPLN [15] and the broad OPG spectrum would lead to a seeding of this Raman peak. The pulse duration of the signal was measured using a 20-GHz digital communication analyzer (HP83480A, Agilent) and a 32-GHz-bandwidth detector (HP83440D, Agilent), giving a FWHM pulse width of 130 ps, which is slightly shorter than the pump pulse as a result of the temporal gain narrowing effect [16]. The corresponding peak power was 20.5 kW. Nevertheless, the broad spectral bandwidth degraded the TBP of the generated signal to 96, which is far from Fourier transform-limited. The broad spectrum from the OPG therefore limits its range of potential applications.

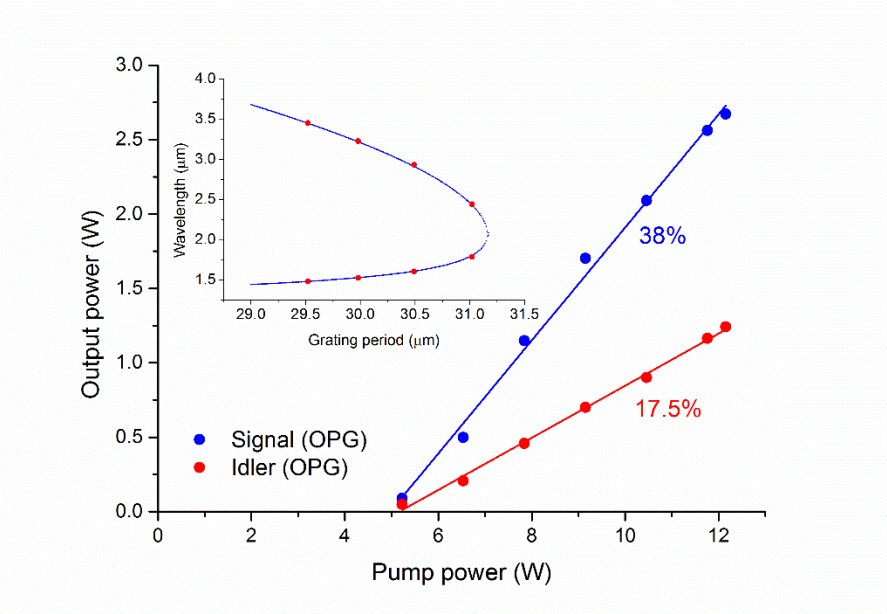

Fig. 2. Signal and idler output power as a function of pump power in OPG operation. The circles are measured data points and the solid lines are linear fits. Inset, the generated signal and idler wavelengths for different PPLN grating periods. The circles represent measured data points and the solid curve is calculated based on Sellmeier data.

In order to narrow the spectral linewidth and, in particular, to improve the degraded TBP, an injection signal was used to seed the OPG for OPA operation. In a first single-pass OPA operation experiment, we employed a commercial fiber-coupled, unpolarized, CW, tunable external-cavity diode laser (Tunics-plus, Photonetics) capable of emitting anywhere in the range 1.5 µm to 1.6 µm with a spectral linewidth of ~100 MHz. The seed and pump beams were combined by a dichroic mirror (DM1, Fig. 1). With 4 mW of seed laser power the pump threshold decreased to approximately 2.5 W. An average signal power of 3.1 W and an average idler power of 1.3 W were obtained at a pump power of only 9.2 W. However, any further increase in the pump power caused damage in the MgO:PPLN crystal. By increasing the pump spot size we could avoid the damage, but this limited the extractable energy as the pump threshold was also increased. As shown in Fig. 3(a), the signal linewidth was reduced to 0.046nm leading to a ~100 times increase in spectral density. Furthermore, the corresponding pulse duration increased to 150 ps, as a consequence of the saturated gain in the OPA operation regime [8], as seen in Fig. 3(b). As a result, the TBP was calculated to be 0.9 which is approximately two times the Fourier limit for Gaussian-shaped pulses (0.44), while the TBP of the pump pulses was 20. Thus the pulse quality of the generated

signal can be effectively improved from that of pump in a seeded OPA process. The attainable signal peak power was thus 20.7 kW at the maximum without damage. The idler spectral FWHM bandwidth was measured to be 6 nm. As expected, the frequency bandwidth was essentially transferred from pump (4.7 cm^{-1}) to idler (5.4 cm^{-1}) [17]. No Raman peaks were observed in this case as the narrower linewidth did not seed its generation.

An exploration of the requirement and influence of the seed laser power on the parametric gain in the single-pass OPA process was performed. With the pump power fixed at 9 W, we measured the signal output power by seeding the OPA at different power levels. As illustrated in Fig. 4(a), with only 2-mW average seed power, saturated maximum extractable power from the OPA can be obtained. Taking into account the duty cycle of the 150-ps pulses and 1-MHz repetition rate, the seed power of 2 mW corresponded to an effective average seed power of only 0.3 μW within the pulse duration and so the 2.7 W output represents a gain of 70 dB. For smaller seed powers gains as high as 79 dB were observed.

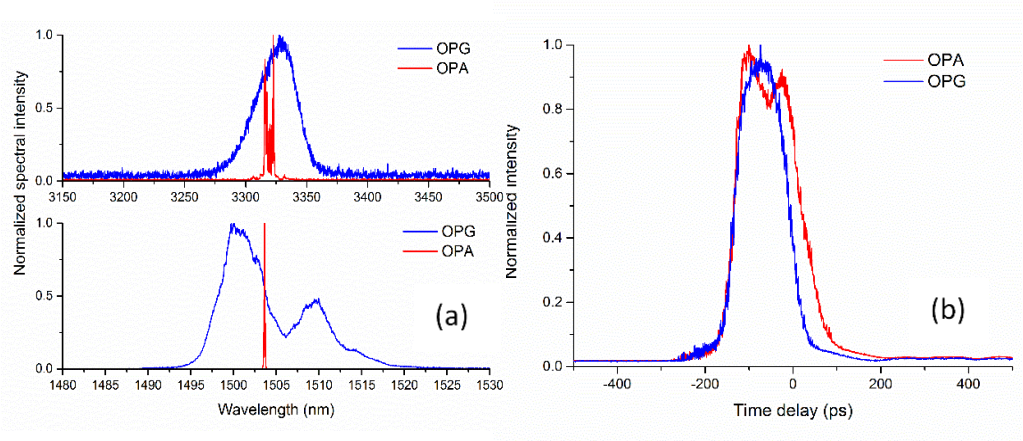

Fig. 3. (a) Spectral measured for signal (below) and idler (on top) in both OPG and OPA operation regime. (b) Signal pulses in OPG and OPA.

The signal beam quality was characterized in both OPG and OPA regimes by using a scanning-slit optical-beam profiler (BP104-IR, Thorlabs). Figure 4(b) shows the experimental results. It can be seen that seeding enhanced the beam quality, with the M^2 factor decreasing from 3.2 for the OPG to 2.1 for the OPA at high signal powers.

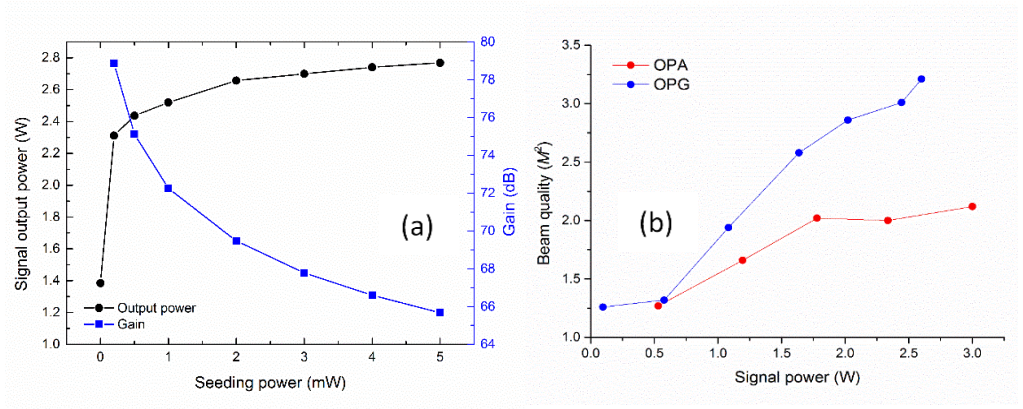

Fig. 4. (a) Signal output power and Gain as a function of different seeding power in OPA. (b) Comparison of measured beam quality (M2) for OPG and OPA.

There was a noticeable increase in parasitic visible radiation in the OPA configuration compared to that of the OPG. As crystal damage had not been observed under OPG operation we speculated that one possible reason for the damage may be related to the narrowed linewidths associated with OPA operation leading to an increase in green-induced infrared absorption [18]. Another possible explanation could be due to self-focusing via cascaded second-order nonlinearity. The high pump intensity of ~0.8 GW/cm^2 indicates that the OPA was operating in the regime where such self-focusing could occur in PPLN [19]. Injecting a seed with more longitudinal modes, associated more quantum noise, would increase the self-focusing threshold [20]. Thus, in order to improve the maximum extractable energy, we reduced the seed spectral density by replacing the narrow-linewidth tunable external-cavity laser with a broader-bandwidth filtered amplified spontaneous emission (ASE) source. The new

seed had a central wavelength of 1541 nm and a FWHM spectral bandwidth of 0.3 nm, and delivered an output power of 24 mW. In order to ensure the two OPAs were operated with exactly the same setup with unchanged alignment, the output power from the second seed was not attenuated but we would expect that much lower average powers would be sufficient to saturate the OPA output power, as shown in the first configuration. With the seed on and pumped at full power, no damage to the PPLN was observed.

Figure 5 shows that the output power of the generated signal and idler increased linearly with slope efficiencies of 40.5% and 18%, respectively, reaching maximum powers of 3.8 W and 1.7 W. The corresponding maximum overall power conversion efficiency was 45% at maximum power and the effective total slope efficiency was 58%. The highest peak power was 25.3 kW for the signal, limited only by the pump power. In the spectral domain, the signal had a spectral bandwidth of 0.33 nm at maximum power, essentially that of the seed, while the idler spectrum had a bandwidth of 8 nm.

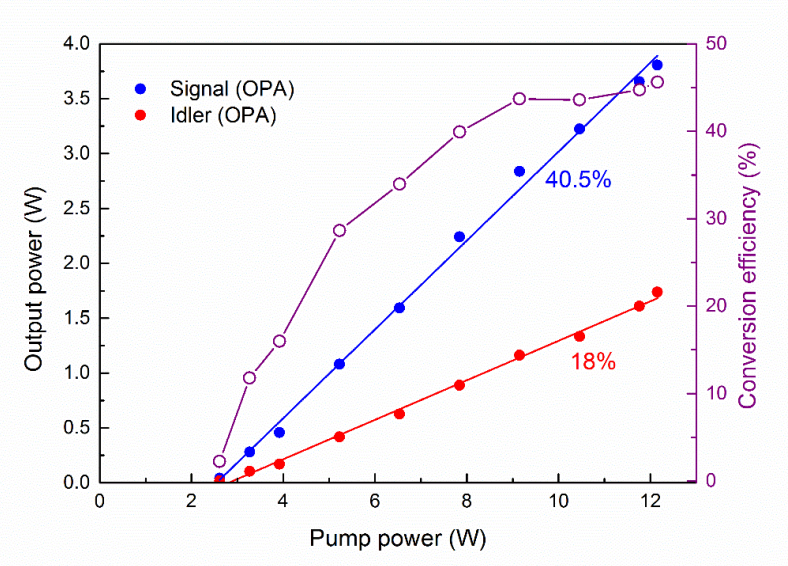

Fig. 5. (Left) Signal and idler output power as a function of pump power in OPA operation with a filtered ASE seed. Circles are measured data points and the solid lines are linear fits. (Right) Total power conversion efficiency versus pump power. The solid line is purely to guide the eye.

4. Conclusions

In summary, we have presented a high-energy, picosecond optical parametric generator based on MgO:PPLN, producing 2.6 μJ and 1.2 μJ signal and idler pulse energies when pumped by a gain-switched-diode-seeded Yb-doped fiber MOPA system employing direct amplification. Seeded with a ~100 MHz linewidth continuous-wave tunable external-cavity laser, pulse energies of 3.1 μJ signal and 1.3 μJ idler have been achieved in a single-pass optical parametric amplifier (OPA). The signal pulse quality in the OPA configuration was significantly improved relative to that of the pump and was just ~2 times transform limited. In order to avoid crystal damage and achieve maximum extractable energy, a broader-bandwidth filtered ASE source seed source with a central wavelength of 1541 nm and a spectral bandwidth of 0.3 nm was employed in a second OPA. A maximum signal energy of 3.8 μJ and idler energy of 1.7 μJ was achieved and the corresponding energy conversion efficiency reached 45%.

Acknowledgments

We would like to acknowledge assistance from Yongmin Jung (ORC, Southampton) to build the narrowband ASE seed source for our work. This work was supported by EPSRC Grant EP/I02798X/1.